THE INCAS PROJECT: AN INNOVATIVE CONTACT-LESS ANGULAR SENSOR

Fabio Giacinto Nardone[(1)], Andrea Di Cintio[(1)], Luca Ghislanzoni[(2)], Giorgio Parzianello[(3)]

[(1)]*CGS S.p.A., via Gallarate 150 – 20151 Milano (Italy), Email: fnardone@cgspace.it, adicintio@cgspace.it*
[(2)]*C-Sigma s.r.l., via Cavour 18 - 23900 Lecco (Italy), Email: info@c-sigma.it*
[(3)]*ESA/ESTEC, Keplerlaan Postbus 299 - 2200 AG Noordwijk (The Netherlands), Email: giorgio.parzianello@aoes.com*

ABSTRACT

Aim of the INCAS project is to develop and qualify a fully redundant Engineering Model of an "INnovative Contact-less Angular Sensor". Positions sensors are largely used in all space telecom missions, including re-entry vehicle and launchers, where mechanisms and pointing scanning devices are required. The main applications are on mechanisms for TeleMeasure (TM) related to the release and deployment and critical deployment of devices or mechanisms as Solar Array Drive Mechanism (SADM) and Antenna Pointing Mechanism (APM).
The INCAS market forecast is therefore related to current potentiometer market and partially to the optical encoder market.

1. INTRODUCTION

The most widely adopted solutions to measure the angular position of a variety of mechanisms on board spacecrafts are based on optical encoders.
However making this type of devices rugged against the severe vibrations environment experienced during launch and against the radiation environment during the flight mission, and extending their operational temperature range, has so far resulted in very expensive products and in some cases to a reduction of the initials requirements due to a real unfeasibility.
Moreover, angular sensors based on potentiometer, an interesting lower cost alternative when the required accuracy is less demanding, are now judged not up to the level of reliability usually required.
In addition, due to current space industry trend requiring substitution of the potentiometer in applications where it is required a long life device, INCAS product will be used in several further applications where the lifetime is the most driving requirement.
With a conservative approach, it is assumed that initially INCAS will be used for applications that require intermediate performance sensors.
There is a real need for an angular sensor, which shall be:

- mechanically robust;
- rugged against radiations;
- insensitive to wide temperature variations under space vacuum conditions;
- inherently low cost.

1.1. HERITAGE

The main starting point of the INCAS project is the output of the ITI-CAS project, carried out by Carlo Gavazzi Space (now CGS S.p.A. an OHB Company) and C-Sigma under an ESA Contract. The outcomes of the ITI-CAS project, which verified the basic performance of the concept for this novel sensor, were presented during the Mechanisms Final Presentation Days at ESA/ESTEC in February 2009.

The novel concept had originally been developed by C-Sigma, for rugged industrial and transportation applications (patent applied for).

2. MAIN FEATURES

The product to be developed is an Absolute Angular Encoder, including Signal Conditioning Electronics, suitable for the space environment, characterized by the following features:

- Self compensating configuration of Hall effect probes;
- Rotary Magnetic Design inherently storing angle position (no stand-by current needed to retain position information);
- Purely analogue signal processing (no software);
- Cost effective;
- Accuracy = ± 0.5°, good repeatability (we expect up to ± 0.1°), and high resolution.

The INCAS absolute encoder aims at satisfying these requirements by means of a contact-less sensor. This is the main characteristic that differentiates the INCAS approach with respect to the current used potentiometers, giving a more robust and reliable solution, especially over long life missions. The low cost approach of this sensor is intended to provide also a convenient alternative to more expensive sensors for this class of performance.
The dedicated electronics shall be fully redundant and all the parts for the Engineering Model prototype, as well as for the Qualification Model foreseen in the next phase, are ITAR free.

'14th European Space Mechanisms & Tribology Symposium – ESMATS 2011'
Constance, Germany, 28–30 September 2011

3. PRINCIPLE OF OPERATION

The principle of operation exploits a biasing permanent magnet generating a magnetic field in an air-gap of suitable geometry, and whose value is a function of angular position. Hall effect probes are located at strategic positions along the air-gap.
The proposed novel design solution consists of using a magnetic circuit configuration such that the angular position is a function of the ratio between the magnetic field values measured by the Hall probes. In this way any drift or degradation of the permanent magnet or Hall probes characteristics is automatically self-compensated. Indeed, the value of said ratio is a function of geometric relationships only, making the sensor insensitive to degradation effects and drift of parameters.

4. INCAS SENSOR DESIGN

The INCAS project started in 2010 and is planned to complete by end of 2011, but it has reached a good development following some initial breadboard tests and analysis.
The sensor is composed of a Stator part and a Rotor part . The Stator will be mated to the flange of the rotary mechanism whose angular position needs to be measured, while the Rotor will be coupled to the shaft of said rotary mechanism.

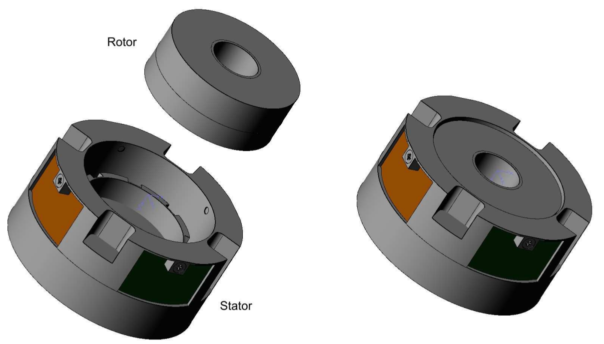

Figure 1 : the complete INCAS Absolute Angular Sensor

	Stator	Rotor
Height	28 mm	15.5 mm
Diameter	58 mm	40 mm
Mass	60-65 g	70 g

Table 1 : stator and rotor characteristics

The Fig. 1 illustrates how the Rotor is completely independent from the Stator, and how the Rotor will be positioned with respect to the Stator.

4.1. Mechanical Design

As general guidelines for the sensor dimensions we have considered the potentiometer usual dimensions and users desiderata.

The Stator performs the following functions :

- it holds firmly in place the Hall Effect Probes along a circle coaxial to the mechanism's shaft main axis;
- it encases the signal processing electronics, properly separating the main electronics from the redundant electronics;
- it provides a circular feature for mating to the mechanism's flange coaxially to the mechanism's shaft main axis.

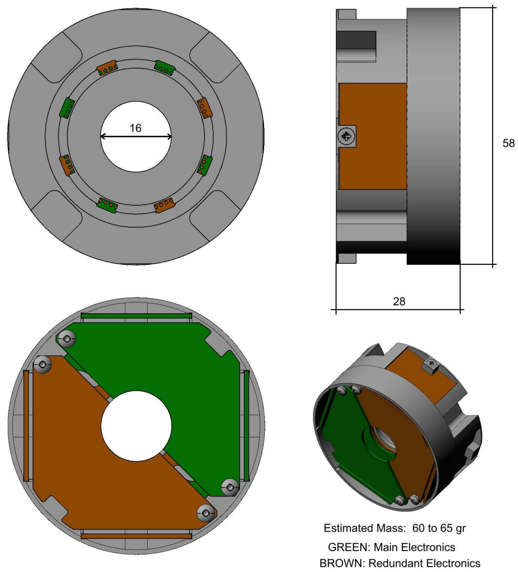

Figure 2 : the Stator (Top, Side, and Bottom views)

The Rotor performs the following functions:

- it holds together all parts of the rotary magnetic circuit;
- it features the circular airgap, whose radial width is a function of angular position;
- it shields the circular airgap from the influence of external magnetic fields, while minimizing the stray fields on the outside;
- it provides means for coupling to the rotary mechanism's shaft.

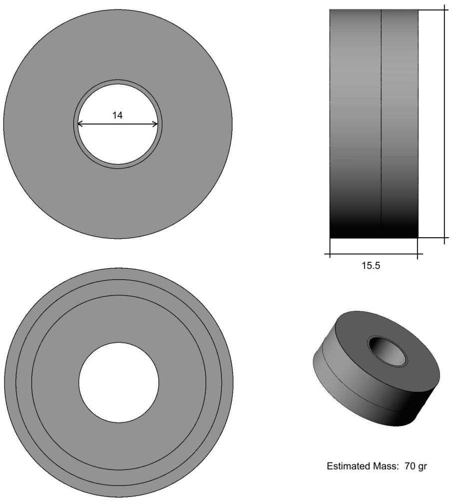

Figure 3 : the Rotor (Top, Side, and Bottom views)

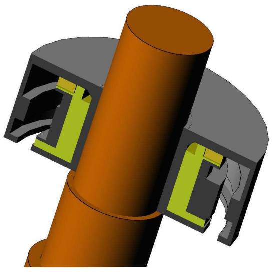

Figure 4 : the Rotor coupled to the Shaft

In order to miniaturize all the sensor we have designed a rigid flex PCB for hosting the electronics.

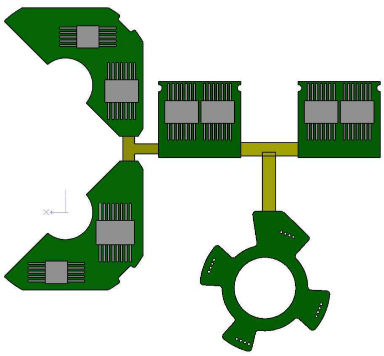

Figure 5 : PCB layout

4.2. Magnetic Design

The following perspective section view illustrates the path followed by the main part of the magnetic flux embracing the circular magnetic circuit implemented in the rotor part of the encoder.

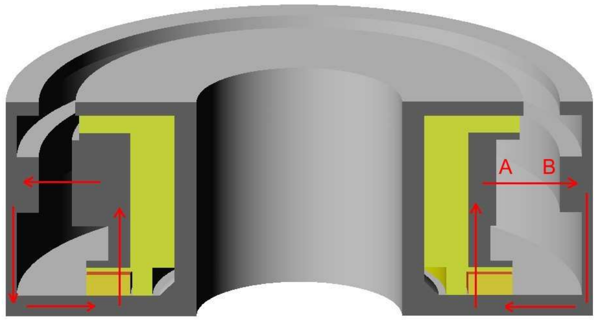

Figure 6 : perspective section view of the rotor's circular magnetic circuit

The Hall probes are located in the airgap delimited by the surfaces A and B (see Fig. 6).

$$B_1 = B(\vartheta) \quad \text{and} \quad B_2 = B(180° + \vartheta) \tag{1}$$

are the two magnetic field values measured by the two Hall probes located at diametrically opposed locations along the circular airgap.

The self-compensating features of the proposed approach are obtained thanks to a particular geometry of the rotary magnetic circuit, and which has been purposely designed so that the magnetic field, $B(\vartheta)$, along its circular airgap possess such a rotational symmetry that for any pair of diametrically opposed locations the respective B field values satisfy the identity:

$$B_1 + B_2 = const \tag{2}$$

function independent from azimuth ϑ

e.g.: a symmetrical triangle, or a cosine function, which both yields

$$f(\vartheta) + f(\vartheta + 180°) = const \tag{3}$$

independent from ϑ

Said self-compensation is then achieved when the angular position reading, ϑ, is obtained as a function g of a function $f(B1, B2)$ with the following form:

$$\vartheta = g\left[f\left(B_1 + B_2\right)\right] \tag{4}$$

where

$$f\left(B_1, B_2\right) = const * \frac{B_1}{B_1 + B_2} \tag{5}$$

4.3. Electronic Design

We developed the electronic design in three stages beginning from the hall probes output :

1. hall probes acquisition through instrumentation amplifier and relative pre-amplification, with feedback loop and temperature compensation;
2. amplification of the two triangle waveform and shifting in phase in order to obtain four triangle waveform useful for achieving the right output waveform;
3. generation of the saw-tooth from the previous waveforms, outputs of the second step.

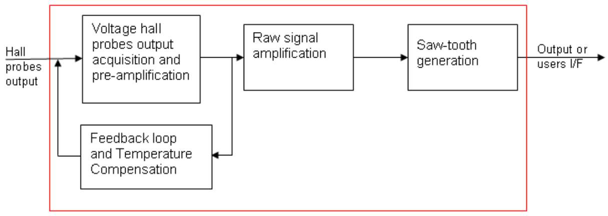

Figure 7 : Electronic design block diagram

4.4. The Self Compensating Principle

The following schematics in Fig. 8 illustrates the solution adopted for obtaining a signal proportional to

$$\frac{B_1}{B_1 + B_2} \tag{6}$$

The trick consists in exploiting the ratiometric characteristics of the Hall Probes, whose gain is proportional to the supply voltage *Vh* , so that for a value B of the magnetic field to be measured the Hall probe output voltage will be proportional to both the value of B, as well as to the value of the supply voltage:

$$V_{out} = K * V_h * B + \frac{V_h}{2} \tag{7}$$

The term *Vh / 2* simply reflects the fact that the Hall probe is designed to generate a zero field output voltage = $V_h / 2$. For positive B values, V_{out} will then be $>V_h / 2$, whereas for negative B it will be $< V_h / 2$.

In our magnetic circuit configuration the Hall probes see only positive B values, we can therefore subtract the value $V_h / 2$, as to refer to 0V the measured value. That is exactly the task of the instrumentation amplifiers INA 1 and INA 2 (see Fig. 8), at whose respective outputs we will hence have :

$$Ch1 = K * V_h * B_1 \quad \text{and} \quad Ch2 = K * V_h * B_2 \tag{8}$$

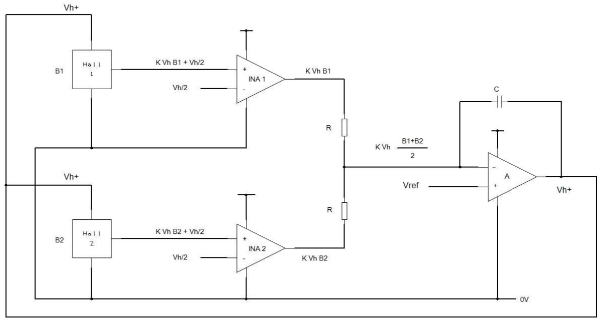

Figure 8 : Signal processing electronic, principle of operation

Their median value,

$$K * V_h * \frac{B_1 + B_2}{2} \tag{9}$$

is then available at the node connecting the two resistors R (we can write this because the two Hall probes are selected from the same lot, as to ensure that they are matched for their K values and corresponding temperature coefficients).

As already explained above, the basic principle of operation requires the ratio :

$$Const * \frac{B_1}{B_1 + B_2} \tag{10}$$

to be calculated with good accuracy.

With the above described circuit it is very easy to obtain a signal of exactly the required form. By choosing a dc gain for the error amplifier, A , of such a large value that it can be considered infinite for all practical purposes (by adopting the classical integrator configuration), the equilibrium equation for the dc operating point simplifies to:

$$K * V_h * \frac{B_1 + B_2}{2} = V_{ref} \tag{11}$$

and which immediately yields:

$$Ch_1 = 2 * V_{ref} * \frac{B_1}{B_1 + B_2} \tag{12}$$

and

$$Ch_2 = 2 * V_{ref} * \frac{B_2}{B_1 + B_2} \tag{13}$$

4.5. Principle of Temperature Compensation

The signal at the output of each Hall Probe features a term proportional to the magnetic fiedl to be measured, *K Vh B*, added to the nominal Zero Field Offset, *Vh /2*, plus its drift with temperature, *drift(T).*

In order to present to the feedback loop a signal proportional solely to *(B1+B2) / 2*, it is necessary to first subtract *Vh/2* and *drift(T).* This is achieved by adding to the negative inputs of the respective INA signals reproducing the respective drift(T). Said *T* compensation signals are obtained by means of resistive networks reading the suitably amplified temperature output of the REF02.

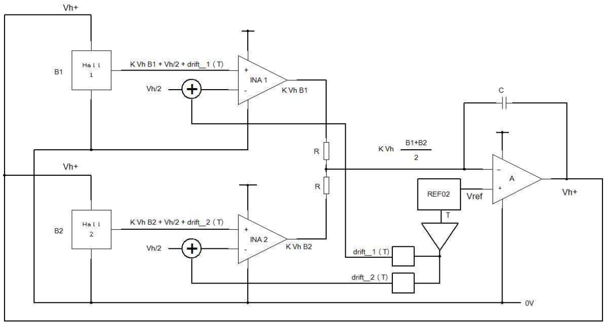

Figure 9 : Principle of operation of the Temperature compensation circuit

4.6. Sawtooth Generation

The output of the first stage of the electronics signal conditioning are two triangle waveform shifted of 90 degree on the complete round of 360 degree, they are the compensated outputs of the two couple of hall probes, that means each waveform is the magnetic field read from a couple of hall probes.

The Fig. 10 shows the two outputs, named CH1 (green one) and CH2 (red one). They are the raw signals pre-amplified, being the outputs of the instrumentation amplifiers already compensated for initial offset voltage and temperature drifts. They are shifted of 90 degree due to the mechanical configuration.

The output sawtooth is then generated by first obtaining, from said two 90° phase shifted triangle waveforms, a total of four triangle waveforms suitably level shifted, and-or inverted, so that their respective central segments (we define a central segment as that part of a triangle's side that corresponds to an arc of 90° centered about its mid point), overlaps to yield a combined linear ramp extending over 4 x 90° = 360°.

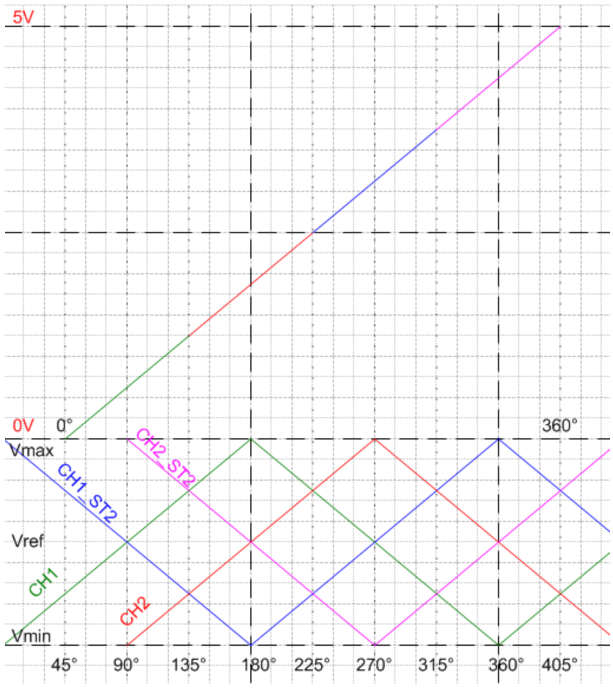

Figure 10 : Sawtooth generation

4.7. Electrical Interface

The following table shows the electrical interfaces of the sensor, identifying input and output signals.

ID	Name	Side	Direction	Remarks
1	Vin	Main	IN	Positive supply voltage (15V)
2	Vout	Main	OUT	Saw-tooth waveform (0-5V)
3	Gnd	Main	OUT	Ground
4	Vref	Main	IN/OUT	Voltage reference
5	Temp	Main	OUT	Temperature
6	Vin	Redundant	IN	Positive supply voltage (15V)
7	Vout	Redundant	OUT	Saw-tooth waveform (0-5V)
8	Gnd	Redundant	OUT	Ground
9	Vref	Redundant	IN/OUT	Voltage reference
10	Temp	Redundant	OUT	Temperature

Table 2 : Electrical interface

5. ANALYSIS PERFORMED

5.1. Magnetic Analysis

In order to assess the sensitivity of the overall encoder accuracy to inaccuracies and assembling tolerances, some Finite Elements Analysis (FEA) simulations were then performed. The software tool utilized for said simulations was:

MAGNUM 3.1, from Field Precision,
http://www.fieldp.com

MAGNUM 3.1 is a FEA solver meant for the 3D design of magnets and permanent-magnet devices, including saturation effects in soft magnetic materials.

Figure 11 : the perspective view of the generated mesh (cross-section plane is the symmetry plane)

The generated mesh was then the input for the MAGNUM 3.1 Magnetostatics 3D FEA Solver.

The output data files generated by MAGNUM 3.1 were then processed using:

MAGVIEW 3.1, from Field Precision

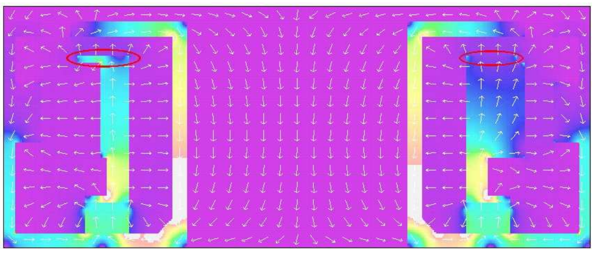

Figure 12 : a slice plot at the symmetry plane.

The simulations were aimed at verifying the sensitivity with regard to radial and axial displacements of the Hall probes with respect to their nominal radial and along-z positions.
Fig. 13 illustrates the resulting % relative error on the ratio B1/(B1+B2) corresponding to a rotor mounted with an eccentricity error of 50 µm in the radial direction (blue line), as well as the error corresponding to 50 µm rotor mounting error along the shaft.
Fig. 14 refers instead to mounting errors of 100 µm.

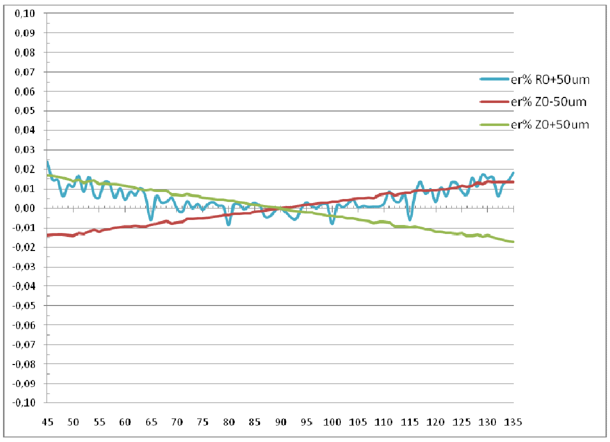

Figure 13 : er% as result of 50um axial and radial displacement

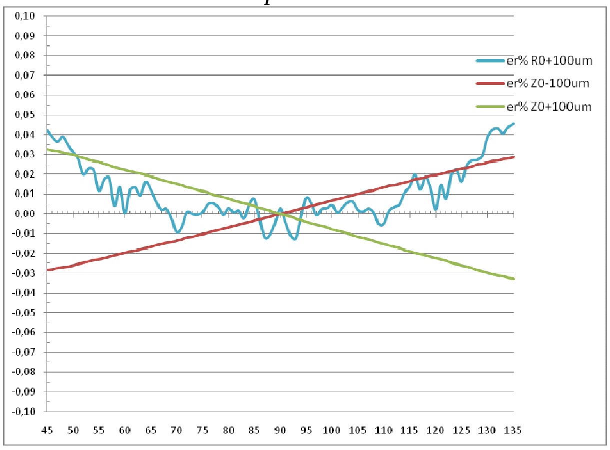

Figure 14 : er% as result of 100um axial and radial displacement

5.2. Structural Analysis

Considering the different materials the thermo-elastic analysis performed on the full specified range of temperature [-50°C : +110°C] has demonstrated the full compliance and high margin of safety.

Part	SFy	SFu	Fty [MPa]	Ftu [MPa]	Applied Stress [MPa]	Type	MoSy	MoSu
430F_Items	1.1	1.25	500	650	262	Von Mises	0.73	0.98
Al 6061-T6 Items	1.1	1.25	241.32	289.58	128	Von Mises	0.71	0.81
Sm2Co17 Magnet	1.1	4	N/A	350	70.5	Von Mises	N/A	0.24
FR4_PCB	1.1	1.25	N/A	275	11.5	Von Mises	N/A	18.13

Table 3 : Margin of safety for thermo-elastic analysis

With regard to the quasi static loads analysis the acceleration of 50g will be applied contemporaneously along the three orthogonal axes.
Also in this case the items have an high margin of safety

Part	SFy	SFu	Fty [MPa]	Ftu [MPa]	Applied Stress [MPa]	Type	MoSy	MoSu
430F_Items	1.1	1.25	500	650	4	Von Mises	112.64	129
Al 6061-T6 Items	1.1	1.25	241.32	289.58	3.3	Von Mises	65.48	69.2
Sm2Co17 Magnet	1.1	4	N/A	350	0.3	Von Mises	N/A	290.67
FR4_PCB	1.1	1.25	N/A	275	2.15	Von Mises	N/A	101.33

Table 4 : Margin of safety for quasi static loads analysis

6. EARLY TEST ON THE BREADBOARD

We have performed thermal tests on a breadboard to verify the self compensating principle and the temperature compensation principle of a reduced circuit (see Fig. 9), with good results.
In term of angular position the results correspond to an absolute deviation contained within

$$\pm 0.15° \text{ over the range } -40°C \text{ to } +120°C$$

It shall be remarked how this result includes the effects of the drift with temperature of :

- the permanent magnet characteristics;
- the magnetic sensitivities of the two Hall probes;
- their respective zero field offsets ;
- the offsets of the two Instrumentation Amplifiers ;
- their respective gains ;
- the value of the REF02 output voltage.

6.1. Lesson Learned

It is fundamental to characterize the hall probes in order to have a good accuracy. In particular the following issues are important:

1. the selection of the hall probe with the most linear dependence from temperature of its zero field offset voltage;
2. the same direction of the linear dependence from temperature, both positive or negative;
3. an accurate matching for each couple supplied by the same feedback loop (see V_h+ in the Fig. 9).

7. PLAN FOR ENVIRONMENTAL TESTS

Environmental tests are foreseen as part of the EQM phase, in order to verify the INCAS sensor environmental characteristics, to have early evidence of eventual troubles and to be ready for the FM qualification.

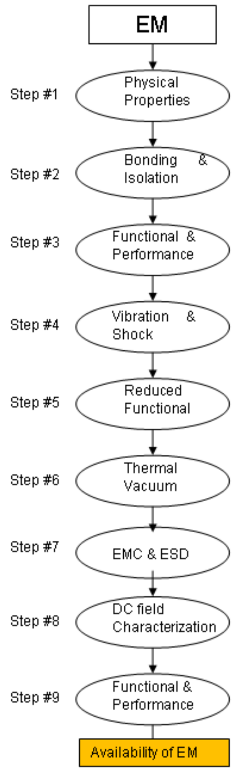

Figure 15 : Flow chart of the test sequence for EM INCAS step by step

In particular the most careful test to be performed shall be the thermal vacuum in order to demonstrate the efficacy of the electronic circuit needed for the compensation.
The test sequence for thermal vacuum tests shall consist in 8 thermal cycles to be carried in a thermal vacuum chamber, at a pressure lower than 1E-5 mbar (see Fig. 16).

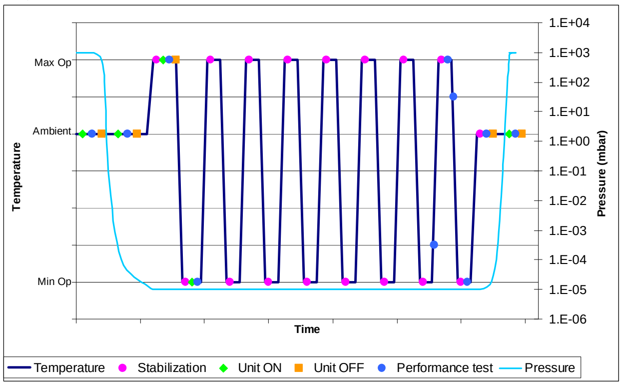

Figure 16 : Test profile for the thermal vacuum test

The full functional tests will be performed :

- Before de-pressurizing the thermal vacuum chamber ;
- After the de-pressurization ;
- At the higher level temperature of the first cycle ;
- At the lower level temperature of the first cycle ;
- Continuous in the last cycle during the rising and falling of the temperature ;
- After the last cycle when the temperature is again stabilized at ambient temperature ;
- At the ambient temperature and ambient pressure, that means after thermal tests.

8. ACKNOWLEDGEMENTS

The INCAS project started in 2010 and is planned to complete by end of 2011. It is running under the ARTES 5.2 program, co-funded by the European Space Agency (ESA).
The follow-on of the activity for the FM development is foreseen under ARTES 3-4 program, still co-funded by the European Space Agency (ESA).

9. REFERENCES

1. Artes 5.2: telecom - technology call for proposals http://emits.esa.int/emits/owa/emits.main.
2. International Patent Application, nr. PCT/IB2009/050167